Morphological and Nanomechanical Behavior of Supported Lipid Bilayers on Addition of Cationic Surfactants

ARTICLE *in* LANGMUIR · JUNE 2013

Impact Factor: 4.46 · DOI: 10.1021/la400067n · Source: PubMed

6 AUTHORS, INCLUDING:

Marina I Giannotti
University of Barcelona
30 PUBLICATIONS **359** CITATIONS
SEE PROFILE

Lorena Redondo-Morata
French Institute of Health and Medical Research
14 PUBLICATIONS **154** CITATIONS
SEE PROFILE

Fausto Sanz
University of Barcelona
190 PUBLICATIONS **2,953** CITATIONS
SEE PROFILE

Langmuir

Article

pubs.acs.org/Langmuir

Morphological and Nanomechanical Behavior of Supported Lipid Bilayers on Addition of Cationic Surfactants

Lia M. C. Lima,[†,‡,§] Marina I. Giannotti,[‡,§,∥] Lorena Redondo-Morata,[‡,§,∥] M. Luísa C. Vale,[†] Eduardo F. Marques,*[,†] and Fausto Sanz*[,‡,§,∥]

[†]Centro de Investigação em Química, Department of Chemistry and Biochemistry, University of Porto, Rua do Campo Alegre, s/n, 4169-007 Porto, Portugal

[‡]Institute for Bioengineering of Catalonia (IBEC), 15-21 Baldiri i Reixac, 08028 Barcelona, Spain

[§]Physical Chemistry Department, University of Barcelona (UB), 1-3 Martí i Franquès, 08028 Barcelona, Spain

[∥]CIBER de Bioingeniería, Biomateriales y Nanomedicina (CIBER-BBN), Campus Río Ebro, Edificio I+D, Poeta Mariano Esquillor, s/n, 50018 Zaragoza, Spain

ABSTRACT: The addition of surfactants to lipid bilayers is important for the modulation of lipid bilayer properties (e.g., in protein reconstitution and development of nonviral gene delivery vehicles) and to provide insight on the properties of natural biomembranes. In this work, the thermal behavior, organization, and nanomechanical stability of model cationic lipid−surfactant bilayers have been investigated. Two different cationic surfactants, hexadecyltrimethylammonium bromide (CTAB) and a novel derivative of the amino acid serine (Ser16TFAc), have been added (up to 50 mol %) to both liposomes and supported lipid bilayers (SLBs) composed by the zwitterionic phospholipid DPPC. The thermal phase behavior of mixed liposomes has been probed by differential scanning calorimetry (DSC), and the morphology and nanomechanical properties of mixed SLBs by atomic force microscopy-based force spectroscopy (AFM-FS). Although DSC thermograms show different results for the two mixed liposomes, when both are deposited on mica substrates similar trends on the morphology and the mechanical response of the lipid−surfactant bilayers are observed. DSC thermograms indicate microdomain formation in both systems, but while CTAB decreases the degree of organization on the liposome bilayer, Ser16TFAc ultimately induces the opposite effect. Regarding the AFM-FS studies, they show that microphase segregation occurs for these systems and that the effect is dependent on the surfactant content. In both SLB systems, different microdomains characterized by their height and breakthrough force F_b are formed. The molecular organization and composition is critically discussed in the light of our experimental results and literature data on similar lipid−surfactant systems.

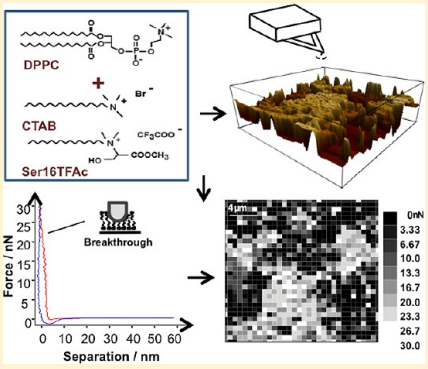

1. INTRODUCTION

Biological lipid-based membranes play a crucial role in a cell's life, controlling the transfer of information between the cell and its environment. These highly complex self-assemblies are mainly composed of membrane proteins and lipids, with the latter organized in a highly fluid bilayer built up of two leaflets with different compositions. Insight on the physicochemical properties of cell bilayers, at the molecular level, is key to an understanding of the specific biological roles that they play.[1−3]

Model membrane systems, such as liposomes, insoluble monolayers, Langmuir−Blodgett films, and supported lipid bilayers, have been extensively used to better understand the structural organization and function of biomembranes, as well as to investigate the membrane activity of diverse compounds, such as surfactants, proteins and drugs. Supported lipid bilayers (SLBs), in particular, are known to correctly mimic biological membranes to a great extent, simplifying the complexity of natural membranes so that the relation between features of individual components, on one hand, and membrane organization and processes, on the other, can be investigated and pinned down. SLBs are relatively easy to prepare leading to planar, well-organized, and stable nanostructures that have been employed in various types of biophysical studies.[4−6] In particular, the effect of various compounds such as proteins,[7,8] drugs,[9,10] and cholesterol[11−13] on the physicochemical properties of lipid bilayers, using SLBs as model systems, has been increasingly explored.

Mixed phospholipid/surfactant bilayers are relevant not only for an understanding of membrane solubilization[14,15] and protein extraction,[16] but also for the development of nonviral gene delivery materials.[17,18] The investigation of the mechanical properties of model lipid bilayers with incorporated cationic surfactants can thus be of great interest for the ultimate design of efficient compaction/transfection vehicles of genetic materi-

Received: January 7, 2013
Revised: May 11, 2013
Published: June 19, 2013

al. Cationic liposomes have the ability to condense and compact DNA and RNA (negatively charged macromolecules), with their amphiphilic behavior allowing for a better crossing of cell membranes.[19,20] The electrostatic condensation of nucleic acids by lipid-based nanostructures leads to tight compaction and subsequent alterations in the surface structure, hydrophobic properties, and size of the macromolecules, hence aiding their internalization in cells. Lipid−nucleic acid colloidal complexes, also called lipoplexes, are known to be less toxic and immunogenic than viral ones, hence offering an alternative path for gene therapy.[17]

The growing demand for biocompatible and biodegradable amphiphiles, both for biomedical and environmental reasons, has required the design of novel specialty compounds. Amino acid-based surfactants are a good alternative to conventional synthetic ones, in particular if they are at least as effective as surface-active agents and if they are able to form aggregates of tailored interest.[21] The synthesis of these "greener" amphiphiles produces molecules with lower toxicity and irritancy toward living organism when compared to usual surfactants.[22] These characteristics have made them an interesting group for applications in the field of pharmaceutics, food, and cosmetics.[23] It is in general the presence of an amino acid residue as the polar headgroup that allows toxicity reduction, with the simultaneous increase in biodegradability.[21,24]

Experimental methods with nanometric resolution, such as atomic force microscopy (AFM)[25] and AFM-based force spectroscopy (AFM-FS),[26] have emerged as powerful tools to probe and characterize the physical properties of lipid bilayers under controlled environmental conditions. AFM-FS provides valuable information on the mechanical properties of SLBs and a direct measurement of the lateral interactions between lipid molecules. In particular, the obtained force−distance curves show a discontinuity that corresponds to the penetration of the AFM tip through the SLBs and is interpreted as the maximum force that the bilayer is able to withstand before breaking, the so-called breakthrough force, F_b. F_b is regarded as a fingerprint of the bilayer stability, and hence, a variation on the physicochemical environment will induce changes in the F_b value. For instance, mixtures of different compounds may yield a separation into different domains of nanometric dimensions, characterized by different values of F_b. The ability to measure both intra- and intermolecular interactions enables the determination of sample elasticity, hardness, adhesion, surface charge densities, and other materials properties.[6,26−29]

The aim of this work has been to investigate the thermal behavior, organization, and nanomechanical stability of model cationic lipid−surfactant bilayers. For these purposes, we used two different cationic surfactants (Figure 1), a common and commercially available one, hexadecyltrimethylammonium bromide (CTAB) and a synthesized derivative of the amino acid serine, *N*-hexadecyl-*N*-(2-hydroxy-1-methyloxycarbonyl)-ethyl-*N*-*N*-dimethylammonium trifluoroacetate (Ser16TFAc).[24] These surfactants were added to both liposomes and SLBs composed of the zwitterionic phospholipid 1,2-dipalmitoyl-*sn*-glycerol-3-phosphocholine (DPPC). We studied the thermal phase behavior of mixed liposomes by differential scanning calorimetry (DSC) and the morphological profiles and nanomechanical properties of mixed SLBs by means of AFM and AFM-FS. Both DPPC/CTAB and DPPC/Ser16TFAc bilayer systems were analyzed in a representative range of compositions up to 50 mol % surfactant, and the observed thermal and mechanical behavior were tentatively correlated with composition and lateral order of each type of segregated domain present in the bilayers.

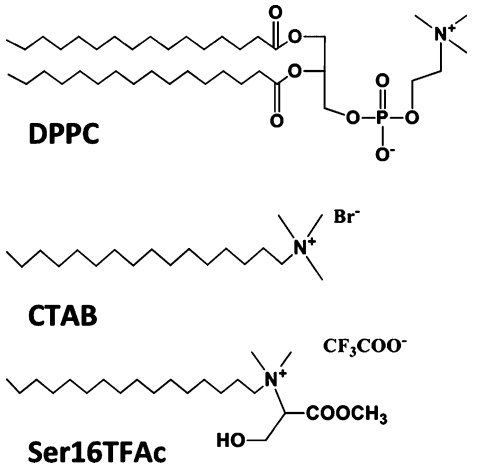

Figure 1. Molecular structure of the studied compounds. 1,2-Dipalmitoyl-*sn*-glycerol-3-phosphocholine (DPPC), hexadecyltrimethylammonium bromide (CTAB), and *N*-hexadecyl-*N*-(2-hydroxy-1-methyloxycarbonyl)ethyl-*N*-*N*-dimethylammonium trifluoroacetate (Ser16TFAc).

2. EXPERIMENTAL SECTION

Materials. 1,2-Dipalmitoyl-*sn*-glycero-3-phosphocholine (DPPC) and hexadecyltrimethylammonium bromide (CTAB) were purchased from Sigma-Aldrich (St. Louis, MO) and used without further purification. The novel cationic serine-based surfactant *N*-hexadecyl-*N*-(2-hydroxy-1-methyloxycarbonyl)ethyl-*N*-*N*-dimethylammonium trifluoroacetate (Ser16TFAc) was synthesized in the Department of Chemistry and Biochemistry, University of Porto, according to a previously reported procedure, and obtained in good purity as ascertained by nuclear magnetic resonance (NMR) and high-resolution mass spectrometry (HR-MS).[24] Chloroform and methanol were purchased from Aldrich, Stemheim, Germany. High purity Milli-Q water, deionized to a resistivity of 18 MΩ cm^{-1}, was used as solvent for all the experiments.

Sample Preparation. DPPC, CTAB, and Ser16TFAc were individually dissolved in chloroform/methanol (3:1) to yield 3 mM stock solutions. Aliquots of DPPC and surfactant solution were mixed with predetermined mole percentage (DPPC/CTAB and DPPC/Ser16TFAc up to 1:1). The composition of the mixtures was calculated as the bulk composition derived from the stock solutions. Then, these solutions were evaporated to dryness under nitrogen flow. Afterwards, warm high purity Milli-Q water (at ca. 60 °C, thus well above the transition temperature of the lipid) was added to achieve a final total concentration of 0.5 mM. Multilamellar vesicles were obtained by subjecting the suspensions to 40 s cycles of vortex mixing and heating (ca. 60 °C). The suspensions were finally subject to sonication for 30 min in a sonicator bath in order to obtain unilamellar liposomes. Circular mica surfaces (Ted Pella, Redding, CA) were used as substrates for AFM experiments and glued onto Teflon discs with epoxy-based mounting glue (Ted Pella, Inc.). In order to obtain planar bilayers, an aliquot of 100 μL of liposome suspension was added to the freshly cleaved mica surface for a deposition time of 30 min at a temperature of ca. 60 °C. After that, the sample was thoroughly rinsed several times with Milli-Q water.

Differential Scanning Calorimetry. DSC measurements were performed using a MicroCal VP-DSC instrument (MicroCal, Northampton, MA). Approximately 600 μL of liposome suspension with a concentration of 10 mM was placed in a sample cell, and the same volume of Milli-Q water was used as reference. The heating and cooling cycles were performed at a scanning rate of 0.5 °C min^{-1} with the temperature range of 70 °C. At least three independent samples were run for each liposome suspension.

dx.doi.org/10.1021/la400067n | *Langmuir* 2013, 29, 9352−9361

Atomic Force Microscopy and Force Spectroscopy. AFM images and FS measurements were performed with a 3D-MFP atomic force microscope (Asylum Research, Santa Barbara, CA). The experiments were performed using V-shaped Si_3N_4 cantilevers with sharp silicon tips (SNL, Bruker, AFM Probes, Camarillo, CA), with a nominal tip radius of 2 nm and a nominal spring constant of 0.35 N m^{-1}. Individual spring constants were calibrated using the equipartition theorem (thermal noise routine)[30] after having correctly measured the piezo sensitivity (V m^{-1}). All AFM images were recorded in intermittent contact mode at room temperature under liquid conditions. The samples were always kept hydrated on the mica-on-glass substrates. Force spectroscopy curves were acquired after imaging the area of interest. Force−distance curves were collected over a 32 × 32 sampling point arrays performed within a range of 2 × 2 to 5 × 5 μm^2 area. Tip velocity was always at 1 $\mu m\ s^{-1}$ with an applied load of 30 nN.

3. RESULTS AND DISCUSSION

3.1. Effect of Cationic Surfactants in DPPC Liposomes: DSC Study. Both CTAB and Ser16TFAc are two single-chained surfactant that form micelles in water, showing Krafft points of 25.0 and 31.2 °C, respectively, and a critical micelle concentration (cmc) of 0.84 mmol·kg^{-1} (at 30 °C) and 0.34 mmol·kg^{-1} (at 40 °C), respectively.[21,31] The addition of these cationic surfactants to DPPC liposomes causes perturbations in the phase behavior of the lipid bilayer. As displayed in Figure 2,

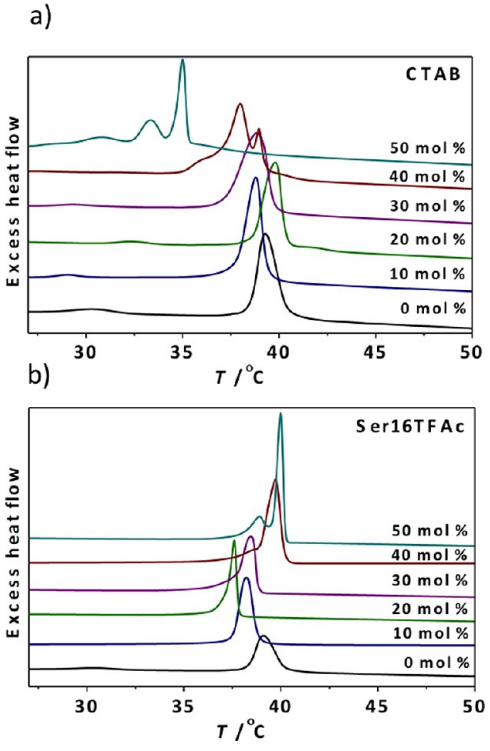

Figure 2. DSC thermograms for DPPC liposome suspensions in Milli-Q water with varying mole percentage of CTAB (a) and Ser16TFAc (b).

neat DPPC liposomes undergo two phase transitions: a weak pretransition (T_p) at 30.3 °C, and a strong and sharp main transition (T_m) at 39.3 °C. The first one corresponds to a change from a tilted gel phase or solid-ordered phase ($L_{\beta'}$) to a rippled gel phase ($P_{\beta'}$), while the second to a change from $P_{\beta'}$ to a liquid-crystalline or fluid phase (L_α).[32]

Upon addition of 10 mol % CTAB to the bilayer, a decrease of T_p to 29.0 °C and of T_m to 38.8 °C is observed (Figures 2a and 3). For 20 mol % CTAB, T_p and T_m increase to 32.3 and

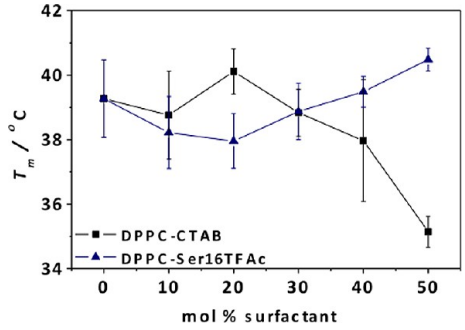

Figure 3. Main phase transition temperature (T_m) of DPPC liposomes as a function of the mole percentage of added surfactant: CTAB (■) and Ser16TFAc (▲).

40.1 °C, respectively, but thereafter, increasing contents of CTAB lead to a gradual decrease of T_m (Figure 3). In fact, for more than 10 mol % in the system, a broad "shoulder" peak appears at lower temperature than the main one. This peak is even more evident for 40 mol %. For 50 mol %, T_m has decreased to about 35 °C, while two other broad peaks are seen at lower temperature. It is clear that, on addition of CTAB, the general trend is that the main peak becomes broader and moves to lower temperature (Figure 3). Hence, the presence of CTAB destabilizes the gel state promoting the fluidity of DPPC bilayers. Moreover, the appearance of the broad additional peaks suggests the formation of lateral domains on the liposome bilayer (of different surfactant−lipid composition), which is intensified as the CTAB content increases. At 50 mol % CTAB, possible assignment of the low-temperature peaks to small mixed aggregates that could form independently from the liposomes is in principle excluded. This is so because micelles do not undergo a gel-to-liquid crystal phase transition. Moreover, any peak associated with the Krafft temperature of CTAB (i.e., the transition from a solid dispersion to micellar solution) should occur at 25 °C, while the lowest temperature peak in the DPPC-CTAB systems appears at 30.9 °C. Furthermore, recent thermal and morphological studies by Correia et al. on DPPC-DTAC mixtures (very similar to those herein studied) have shown that up to surfactant molar fractions of 0.5 only mixed liposomes are present, while mixed micellar aggregates (disks, threads and spheres) appear only at about 0.7 and beyond.[33]

A somewhat different behavior is observed when one adds the cationic surfactant Ser16TFAc onto DPPC liposomes (Figure 2B). The presence of 10 and 20 mol % Ser16TFAc lowers the T_m of DPPC to 38.2 and 37.9 °C, respectively, inducing fluidity on the bilayer. However, for higher Ser16TFAc contents, T_m starts rising again, becoming at 40 and 50 mol % higher than the value for neat DPPC bilayers and probably inducing some molecular ordering in the bilayer (Figure 3). Besides, from 20 mol % on, a shoulder peak starts growing to the left of the main peak until it becomes a clear (coalesced) peak at 50 mol %. The pretransition of neat DPPC seems to be abolished in the presence of Ser16TFAc. A fluidization of the DPPC bilayer is observed only at low Ser16TFAc contents (up to about 30 mol %) and then, for

dx.doi.org/10.1021/la400067n | Langmuir 2013, 29, 9352−9361

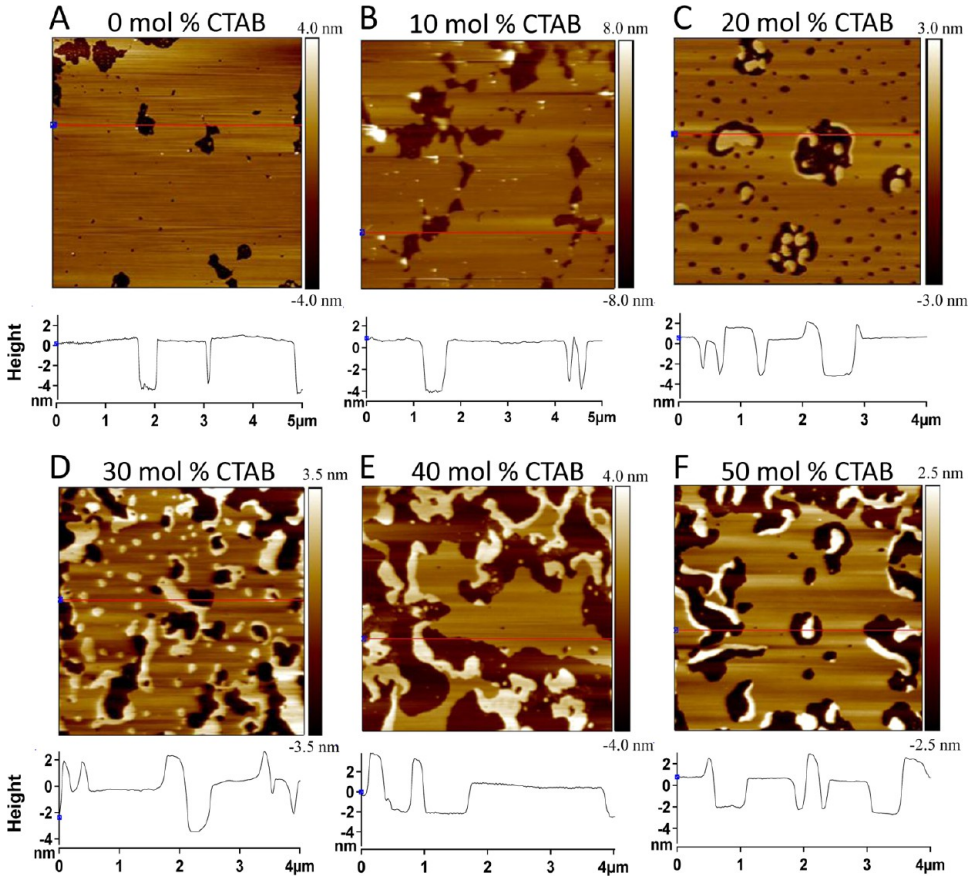

Figure 4. AFM intermittent contact mode topographical images and the corresponding height profiles for various CTAB mole percentages in DPPC/CTAB SLBs in Milli-Q water at room temperature: (A) 0 mol % (scan size 5 μm); (B) 10 mol % (scan size 5 μm); (C) 20 mol % (scan size 4 μm); (D) 30 mol % (scan size 4 μm); (E) 40 mol % (scan size 4 μm); (F) 50 mol % (scan size 4 μm).

increasing contents, a structuring effect (thermal stabilization of the gel phase) is observed.

The different behavior in the presence of these two surfactants may be due to a different surfactant partitioning between the lipid and aqueous phases. While the so-called *strong* surfactants solubilize lipid membranes at surfactant-to-lipid molar ratios below 50 mol %, *weak* surfactants accommodate in the membrane up to surfactant-to-lipid ratios above 1:1 before the bilayer collapses.[34] Even though both systems show different trends, the formation of domains of different composition seems to be the main feature of these mixed surfactant−lipid bilayers, especially at high surfactant content.

3.2. Incorporation of CTAB on DPPC Supported Bilayers. To investigate the influence of CTAB on DPPC SLBs, samples with different mole percentage of added surfactant were imaged and nanomechanically characterized by AFM-FS. Figure 4A shows a topographic image of a supported DPPC bilayer with a thickness of about 4.9 ± 0.3 nm, a value that is in agreement with previous studies.[35,36] On addition of 10 mol % CTAB, a similar topography with a height of 5.3 ± 0.5 nm is observed (Figure 4B). However, when higher CTAB contents are introduced, two distinct domains are formed on the bilayer: higher domains with an average of 5.3 nm and lower ones with an average of 3.1 nm (Figure 5). The continuous region is the lower structure, whereas the higher domains are mostly distributed on the edges of the thinner layer. Thus, while the DPPC/CTAB SLB is fully miscible on

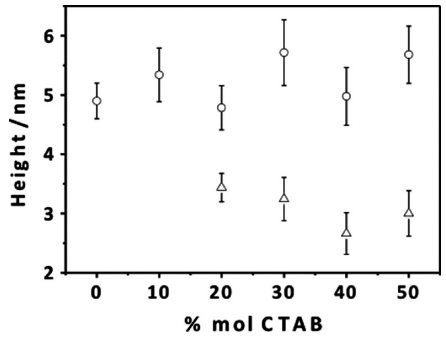

Figure 5. Average heights of the different domains observed in DPPC/CTAB SLBs as a function of mole percentage of CTAB: (○) higher features; (△) lower features. Each height value is an average from 30 measurements on the section profile from the AFM images.

incorporation of 10 mol % CTAB, two different types of domains clearly coexist at higher surfactant contents. The decrease in the height of the bilayer upon addition of 10−20 mol % CTAB may suggest that the bilayer undergoes a phase transition from gel to liquid-crystalline state. However, no drop of the phase transition temperature below room temperature was detected for the vesicle suspensions. On the basis of the thickness of the domains, one can presume that the higher domains are essentially DPPC-rich domains while the lower ones are CTAB-rich domains (in fact, a thickness of about 3.0 nm for adsorbed CTAB bilayers has been previously reported by Cao and Wang).[37]

dx.doi.org/10.1021/la400067n | *Langmuir* 2013, 29, 9352−9361

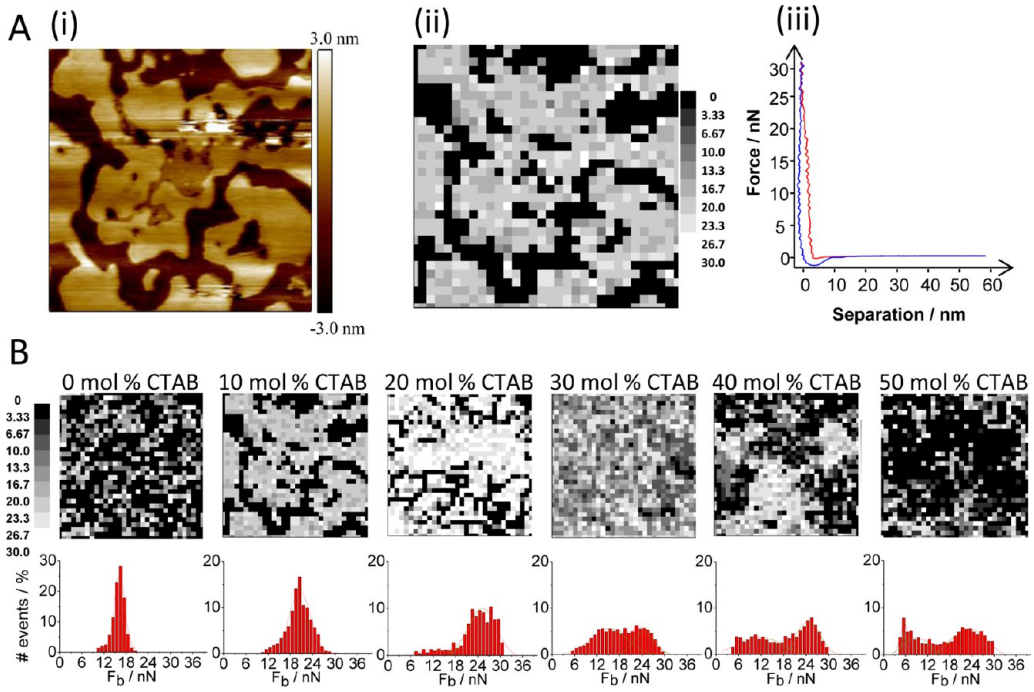

Figure 6. (A) DPPC/CTAB SLB with 10 mol % CTAB in Milli-Q water at room temperature: (i) Intermittent contact mode topographical image, (ii) the corresponding map of F_b values, (iii) typical force−distance curve of the lipid bilayer mixture (red, approach event; blue, retract event). (B) Maps and distributions of F_b values of DPPC/CTAB for various CTAB mole percentages. Scan sizes are 3 μm for 0, 10, and 40 mol % CTAB and 4 μm for 20, 30, and 50 mol % CTAB.

To assess the nanomechanical behavior of the distinct domains, AFM-FS was performed by measuring the maximum force that the bilayer is able to withstand before breaking (breakthrough force, F_b). AFM-based force mapping, consisting in an array of force curves recording the spatial position, coupled with AFM imaging, provides a direct correlation of the different morphologies with their mechanical response.[38] This allows the study of the mechanical properties of each microdomain for a defined area, as exemplified for 10 mol % CTAB in Figure 6A. It is clear that the distinct types of domain have a different mechanical behavior. Higher domains exhibit higher F_b values than the lower domains.

Figure 6B shows the maps and the distributions of F_b values for each CTAB molar fraction on DPPC SLBs. For neat DPPC bilayers in water, an average force of 16.2 ± 0.1 nN is needed to puncture the bilayer, a value that is in agreement with previous studies.[26] As 10 mol % CTAB is incorporated in the system, the yield threshold force values shift to 21.0 ± 0.1 nN with a wider distribution. The presence of 20 and 30 mol % CTAB induces a bimodal F_b distribution with mean values of 12.4 ± 2.7 and 25.3 ± 0.3 nN for 20 mol %, and 15.1 ± 0.4 and 24.5 ± 0.2 nN for 30 mol %, each F_b for the different domains observed in the topographic images (Figure 4). These values further support the absence of a gel-to-liquid crystal transition upon addition of 20 mol % CTAB, as mentioned above, since a liquidlike bilayer is known to give breakthrough force values in the order of a few nN.[13] However, when 40 and 50 mol % CTAB are introduced, a trimodal F_b distribution is observed. The mean values are 6.7 ± 0.5, 10.2 ± 0.9, and 23.7 ± 0.4 nN for 40 mol % and 7.3 ± 0.4, 12.5 ± 0.2, and 23.3 ± 0.5 nN for 50 mol %. As can be seen in Figure 7, from 20 mol %, the higher average F_b (24−25 nN) remains roughly constant as CTAB is further added. With somewhat higher dispersion in the values (12−15 nN), the same appears to happen to the lower breakthrough force, while

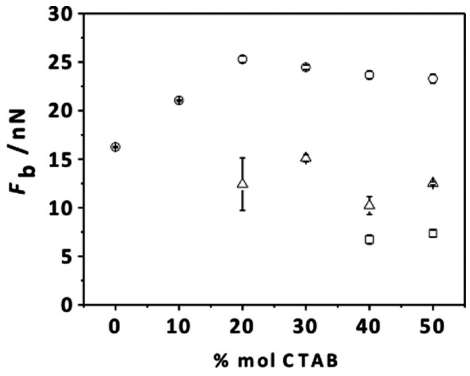

Figure 7. Mean distribution of breakthrough forces (F_b) at room temperature for DPPC/CTAB SLBs as function of mole percentage of CTAB: (○) high F_b domains; (△) intermediate F_b domains; (□) low F_b domains.

at 40 and 50 mol % a third and even smaller F_b value is apparent.

In line with what was mentioned above, these results suggest that higher features, which also show higher F_b, can probably be ascribed to essentially DPPC-rich domains, while lower features, with lower F_b, probably correspond to CTAB-rich domains. The roughly constant average F_b for the DPPC-rich domains further suggests that the addition of more CTAB will change the relative amount of each domain type, generating more CTAB-rich domains to the detriment of DPPC-rich ones (only a more in-depth statistical study of different images might shed light in this interesting point, but this is outside the scope of the current study). The smallest average F_b (around 7 nN) found for 40 and 50 mol % is most likely associated with regions basically composed by neat CTAB (presumably some type of adsorbed micellar-like aggregates) that appear when the

dx.doi.org/10.1021/la400067n | Langmuir 2013, 29, 9352−9361

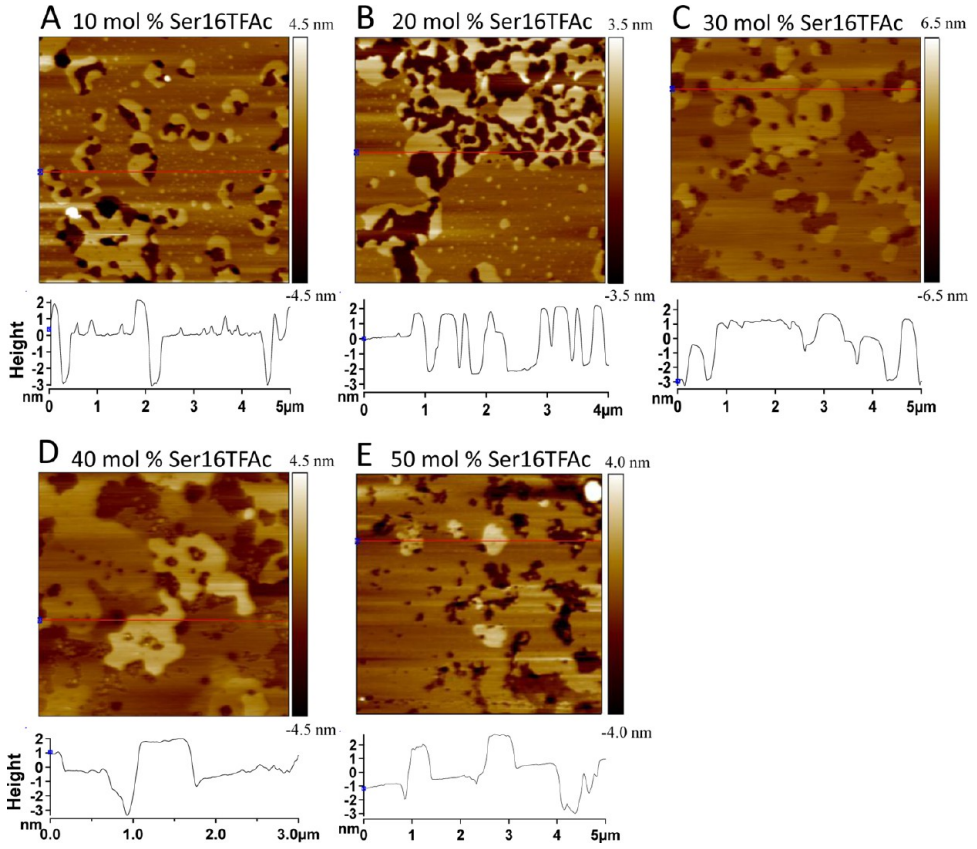

Figure 8. AFM intermittent contact mode topographical images and the corresponding height profiles for various Ser16TFAc mol % in a DPPC/Ser16TFAc SLB in Milli-Q water at room temperature: (A) 10 mol % (scan size 5 μm); (B) 20 mol % (scan size 4 μm); (C) 30 mol % (scan size 5 μm); (D) 40 mol % (scan size 3 μm); (E) 50 mol % (scan size 5 μm).

content of cationic surfactant reaches a high enough value.[39] Although the existence of a third microdomain is not directly evidenced for 40 and 50 mol % from the topographic images, when a systematic analysis of F_b events is performed over the same area, a trimodal F_b distribution is indeed observed.

Comparison of these results on SLBs with DSC experiments for DPPC/CTAB liposomes indicates that, in both cases, when the cationic surfactant is added, microdomains are formed in the bilayers, with different characteristics between them. Moreover, there is presence of DPPC-rich domains in the mixed bilayers, manifested by greater height, higher average F_b, and the main endothermic peak in DSC. However, these results are not in complete agreement since an increase of the nanomechanical stability is observed until 20 mol %, with the subsequent permanency of F_b values for higher contents, while DSC shows an increasing fluidity in the system. These differences are not surprising and have also been reported in previous studies.[13] One has to take into account that, in comparison with bulk liposomes, the mica substrate of SLBs can affect the lipid ordering and compaction as well as the domain composition.[40]

3.3. Incorporation of Ser16TFAc on DPPC Supported Bilayers. The incorporation of the surfactant Ser16TFAc on DPPC bilayers also induces the formation of distinct domains (Figure 8). Unlike the case of DPPC/CTAB mixtures, two different domains already coexist with only 10 mol % Ser16TFAc, probably representing an early stage of a bilayer/micelle-like domain coexistence. As the content increases, the segregated domains are continuously observed, due to a higher immiscibility of the system, as indicated before by the DSC results. The average height is approximately 4.9 nm for the higher domains and approximately 3.0 nm for the lower domains (Figure 9). For DPPC/Ser16TFAc with 40 mol %

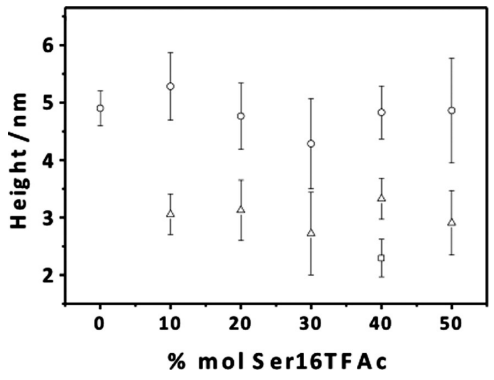

Figure 9. Average heights of the different domains observed in DPPC/Ser16TFAc SLBs: (○) higher features; (△) intermediate features; (□) lower features.

Ser16TFAc, the topographic images clearly reveal the segregation of a new domain with an average height of 2.3 ± 0.3 nm (Figure 8D), probably meaning that the maximum amount of Ser16TFAc that the second domain can incorporate has been reached, thus promoting formation of three distinct types of microdomains. It is also observed that the higher domains are always embedded in the lower ones. Like in the DPPC/CTAB mixture, these distinct regions can probably be

dx.doi.org/10.1021/la400067n | Langmuir 2013, 29, 9352−9361

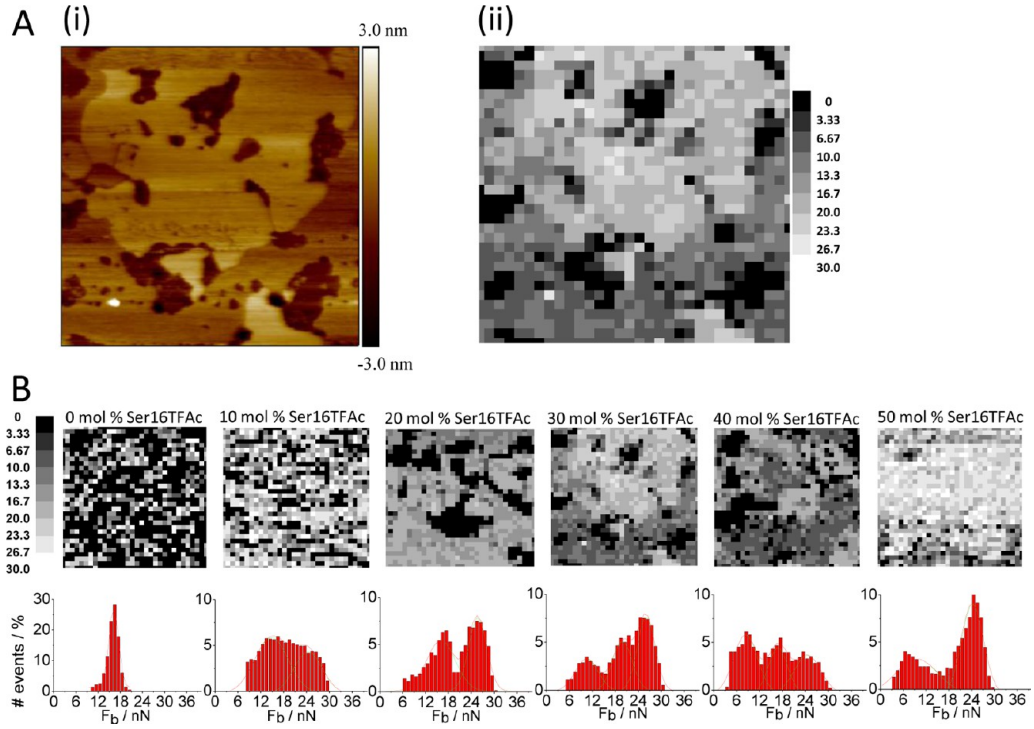

Figure 10. (A) DPPC/Ser16TFAc SLBs with 30 mol % Ser16TFAc in Milli-Q water at room temperature: (i) intermittent contact mode topographical image and (ii) the corresponding map of F_b values. (B) Maps and distributions of F_b values of DPPC/Ser16TFAc SLBs for various Ser16TFAc mole percentages. Scan sizes are 4 μm for 10 and 50 mol % and 3 μm for 0, 20, 30, and 40 mol % Ser16TFAc.

ascribed to a DPPC-rich domain and to Ser16TFAc-rich domains.

AFM-FS experiments were performed on the DPPC/Ser16TFAc SLBs in order to directly correlate the distinct domains with their nanomechanical strength. Figure 10A demonstrates an example of a 30 mol % Ser16TFAc topographic image and the corresponding map of F_b. Just as observed in the DPPC/CTAB system, the higher features correspond to higher F_b and the lower features exhibit smaller F_b values. The distributions and maps of F_b for each Ser16TFAc molar fraction are represented in Figure 10B. When 10 and 20 mol % Ser16TFAc are introduced in the system, two distinct distributions are observed, with mean F_b values of 24.6 ± 0.8 and 15.0 ± 0.7 nN for 10 mol %, and 25.6 ± 0.8 and 16.0 ± 0.5 nN for 20 mol %. The higher F_b values of each composition are always above the average F_b value for neat DPPC (16.2 ± 0.1 nN). However, contrary to what happens with the DPPC/CTAB system, the incorporation of 30 mol % Ser16TFAc leads to the formation of a trimodal distribution, with average values of 26.2 ± 0.3, 20.0 ± 0.5, and 10.3 ± 0.3 nN. For 40 mol %, the same behavior is observed, with comparable F_b values of 24.6 ± 0.3, 16.7 ± 0.2, and 8.8 ± 0.1 nN. This situation changes when the Ser16TFAc content is increased up to 50 mol %. Again, two segregated domains are observed in the system, with mean values of 24.1 ± 0.2 and 9.3 ± 0.8 nN, in line with the topographic images.

As previously discussed, despite that for 30 mol % a two-phase system is observed on the topographic images, three distributions of F_b are obtained when the SLB is continuously punctured. Equally to the DPPC/CTAB system, a roughly constant value of the higher F_b is attained, as well as a clear formation of regions with lower F_b, as can be followed in Figure 11. Again, this suggests some saturation level of Ser16TFAc molecules in the presumptive DPPC-rich regions, with

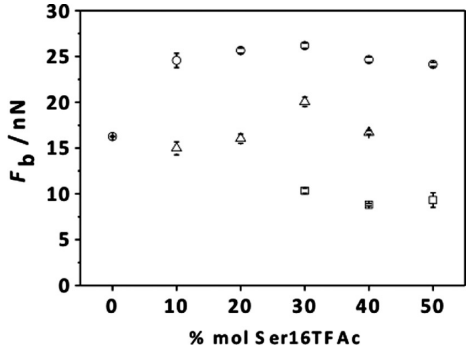

Figure 11. Mean distribution of breakthrough forces at room temperature for DPPC/Ser16TFAc SLBs. (○) High breakthrough force domain; (△) intermediate breakthrough force domain; (□) low breakthrough force domain.

formation of regions with the excess surfactant molecules. It is worth mentioning that the intermediate F_b distributions of the diverse Ser16TFAc contents have mean values nearly identical to the F_b of neat DPPC (Figure 11). Moreover, the higher features on the topographic images of the different contents show heights similar to that of neat DPPC bilayers (Figure 9). This again highlights that when Ser16TFAc is introduced, DPPC immediately saturates and rejects surfactant molecules forming distinct domains and leading to numerous regions mostly constituted of DPPC.

Despite the fact that the bilayer properties probed by DSC and AFM are different, because of the effect of the substrate-lipid interactions on the SLBs, both techniques demonstrate qualitatively the same trend of microphase separation. For both cases, the broadening of the peaks at lower temperatures with only 20 mol % suggests already the incipient formation of microheterogeneities in the system, which will give rise to a

dx.doi.org/10.1021/la400067n | Langmuir 2013, 29, 9352−9361

split in two DSC peaks at higher surfactant content. Thus, the incipient formation of an additional broad peak in the DSC thermograms for both surfactants, at 40 mol % in CTAB and at 30 mol % in Ser16TFAc, can be qualitatively correlated with the AFM-FS experiments, which show segregation of the components into three distinct regions with different F_b, which may have different thermal transition temperatures. In the case of mixtures at 10 mol %, for both CTAB and Ser16TFAc, one observes a unique peak in the DSC thermograms, at very similar temperatures. However, in the AFM topography observations and nanomechanical analysis, there is one phase in the case of 10 mol % CTAB and two different phases coexisting in the case of 10 mol % Ser16TFAc. Despite the influence of the hard underlying substrate in the case of the SLBs, as it has been previously mentioned, this could be an indicator that the AFM technique, specially the nanomechanical characterization, can reveal extra information regarding the interplay between the PC lipid and the two different surfactants.

Incorporation of both surfactants on the DPPC bilayer leads to an increase of the nanomechanical stability of the bilayers up to 20 mol % for CTAB and up to 10 mol % for Ser16TFAc. Afterward, an approximately constant value of F_b and the formation of lower F_b distributions corresponding to distinct domain types are observed. In this respect, Gurtovenko et al. have shown by molecular dynamics simulations that the influence of the cationic dimyristoyltrimethylammonium propane lipid (DMTAP) on dimyristoylphosphatidylcholine (DMPC) bilayers (systems similar to ours) is mostly governed by headgroup interactions.[41] With the addition of small DMTAP mole percentage, the orientation of PC dipoles leads to a reduction of the average area per molecule and subsequently to a compression of the bilayer. However, when a certain molar fraction ($x_{DMTAP} \approx 0.75$) is reached, the enhancement of the repulsive electrostatic interactions between DMTAP headgroups forces an expansion of the bilayer. Our results seem to be consistent with these studies. The incorporation of small mole percentages of each cationic surfactant on DPPC SLBs increases the force needed to puncture the bilayer, and this can be due to a denser packing of the bilayer due to electrostatic interactions between the cationic surfactant headgroup and the choline charge of the phospholipid headgroup. However, already at 20 mol % for CTAB and 10 mol % for Ser16TFAc, a "saturated" system is attained and phase-segregates into new domains, the putative surfactant-rich domains, which have smaller F_b values perhaps due to the repulsive electrostatic interactions between surfactant headgroups, which do not favor close packing. Most probably, the limiting molar fraction saturation for CTAB is higher than Ser16TFAc because of the less bulky trimethylammonium headgroup (Figure 1) which favors closer interaction with the DPPC zwitterionic headgroup. Other molecular dynamics studies have also shown an increase on the organization of PC bilayers on addition of cationic surfactants.[42−44] The cationic surfactants differ only in headgroup composition (having identical chain composition and length), but this structural difference is enough to induce some significant differences in the way the surfactants interact with DPPC bilayers.[44,45]

4. CONCLUSIONS

In this work, we have shown that both cationic surfactants CTAB and Ser16TFAc have a marked effect on the thermal behavior, organization, and nanomechanical stability of DPPC bilayers. Mixed DPPC−surfactant liposomes have been analyzed by DSC and mixed supported bilayers by AFM imaging and AFM-FS, in the range of up to 50 mol % surfactant. Both SLB systems show formation of distinct domains for increasing surfactant contents, each one with a characteristic F_b value, in qualitative agreement with DSC results. DSC data revealed the existence of relevant differences in the interaction of these structurally similar surfactants with DPPC liposomes. CTAB seems to decrease the degree of organization on the bilayer, while Ser16TFAc induces, in general, the opposite effect.

By means of AFM imaging and AFM-FS studies, microphase segregation for DPPC/CTAB system is observed for contents higher than 20 mol %, while for the system DPPC/Ser16TFAc it occurs with only 10 mol %. Up to these contents, an increase of the F_b values is also observed in both systems. However, when higher contents are added, an approximately constant distribution of F_b is reached. The higher F_b is attributed to putative DPPC-rich domains while lower F_b values are attributed to surfactant-rich domains. The latter are mechanically less stable showing regions with lower heights at the topographic images. In the case of CTAB, from 40 mol % a third F_b distribution is observed. For Ser16TFAc, the appearance of the third F_b value occurs at 30 mol %. Although DSC thermograms show different results for the two liposomes mixtures, when both are deposited on mica substrates, similar trends on the morphology and the mechanical response are observed.

Our results elucidate how these two structurally similar cationic surfactants interact with DPPC bilayers. In our view, this type of studies is relevant for the general understanding of the modulation of lipid bilayer properties and also for the development of cationic lipid assemblies used in gene delivery.

AUTHOR INFORMATION

Corresponding Author

*E-mail: efmarque@fc.up.pt (E.F.M.); fsanz@ub.edu (F.S.).

Notes

The authors declare no competing financial interest.

ACKNOWLEDGMENTS

L.M.C.L. gratefully acknowledges the Erasmus Mobility Program and CIBER-BBN for financial support. E.F.M. and M.L.C.V. gratefully acknowledge financing from FEDER through Programa COMPETE and national funding from FCT, Fundação para a Ciência e Tecnologia, under Projects PEST-C/QUI/UI0081/2011 and PTDC/QUI-QUI/115212/2009. M.I.G., L.R.-M., and F.S. acknowledge the financial support from Agència de Gestió d'Ajuts Universitaris i de Recerca (AGAUR) through 277SGR2009, from Ministry of Economy and Competitiveness by Grant CTQ2011-25156 and CIBER-BBN. CIBER-BBN is an initiative funded by the VI National R&D&i Plan *2008-2011, Iniciativa Ingenio 2010, Consolider Program, CIBER Actions* and financed by the Instituto de Salud Carlos III with assistance from the *European Regional Development Fund*. We acknowledge Dr. G. Oncins from Nanometric Techniques Unit of the Scientific and Technical Center of the University of Barcelona (CCiTUB) for technical support. Thanks are also due to Sandra Goreti Silva for help with the synthesis of compound Ser16TFAc.

REFERENCES

(1) Simons, K.; Vaz, W. L. C. Model systems, lipid rafts, and cell membranes. *Annu. Rev. Biophys. Biomol. Struct* **2004**, *33*, 269−295.

(2) Lipowsky, R.; Sackmann, E. *Structure and dynamics of membranes*; Elsevier: Amsterdam, 1995; Vol. *1*.

(3) Muller, D. J. AFM: A nanotool in membrane biology. *Biochemistry* **2008**, *47*, 7986−7998.

(4) El Kirat, K.; Morandat, S.; Dufrêne, Y. F. Nanoscale analysis of supported lipid bilayers using atomic force microscopy. *Biochim. Biophys. Acta, Biomembr.* **2010**, *1798*, 750−765.

(5) Johnston, L. J. Nanoscale imaging of domains in supported lipid membranes. *Langmuir* **2007**, *23*, 5886−5895.

(6) Canale, C.; Jacono, M.; Diaspro, A.; Dante, S. Force spectroscopy as a tool to investigate the properties of supported lipid membranes. *Microsc. Res. Tech.* **2010**, *73*, 965−972.

(7) Chen, S. F.; Zheng, J.; Li, L. Y.; Jiang, S. Y. Strong resistance of phosphorylcholine self-assembled monolayers to protein adsorption: Insights into nonfouling properties of zwitterionic materials. *J. Am. Chem. Soc.* **2005**, *127*, 14473−14478.

(8) Mueller, H.; Butt, H. J.; Bamberg, E. Adsorption of membrane-associated proteins to lipid bilayers studied with an atomic force microscope: Myelin basic protein and cytochrome *c*. *J. Phys. Chem. B* **2000**, *104*, 4552−4559.

(9) Berquand, A.; Mingeot-Leclercq, M. P.; Dufrêne, Y. F. Real-time imaging of drug-membrane interactions by atomic force microscopy. *Biochim. Biophys. Acta, Biomembr.* **2004**, *1664*, 198−205.

(10) Leonenko, Z.; Finot, E.; Cramb, D. AFM study of interaction forces in supported planar DPPC bilayers in the presence of general anesthetic halothane. *Biochim. Biophys. Acta, Biomembr.* **2006**, *1758*, 487−492.

(11) Crane, J. M.; Tamm, L. K. Role of Cholesterol in the Formation and Nature of Lipid Rafts in Planar and Spherical Model Membranes. *Biophys. J* . **2004**, *86*, 2965−2979.

(12) Sullan, R. M. A.; Li, J. K.; Hao, C.; Walker, G. C.; Zou, S. Cholesterol-Dependent Nanomechanical Stability of Phase-Segregated Multicomponent Lipid Bilayers. *Biophys. J* . **2010**, *99*, 507−516.

(13) Redondo-Morata, L.; Giannotti, M. I.; Sanz, F. Influence of Cholesterol on the Phase Transition of Lipid Bilayers: A Temperature-Controlled Force Spectroscopy Study. *Langmuir* **2012**, *28*, 12851−12860.

(14) Almgren, M. Mixed micelles and other structures in the solubilization of bilayer lipid membranes by surfactants. *Biochim. Biophys. Acta, Biomembr.* **2000**, *1508*, 146−163.

(15) Heerklotz, H.; Binder, H.; Lantzsch, G.; Klose, G.; Blume, A. Lipid/detergent interaction thermodynamics as a function of molecular shape. *J. Phys. Chem. B* **1997**, *101*, 639−645.

(16) Garavito, R. M.; Ferguson-Miller, S. Detergents as Tools in Membrane Biochemistry. *J. Biol. Chem.* **2001**, *276*, 32403−32406.

(17) De Laporte, L.; Cruz Rea, J.; Shea, L. D. Design of modular non-viral gene therapy vectors. *Biomaterials* **2006**, *27*, 947−954.

(18) Khalil, I. A.; Kogure, K.; Akita, H.; Harashima, H. Uptake pathways and subsequent intracellular trafficking in nonviral gene delivery. *Pharmacol. Rev.* **2006**, *58*, 32−45.

(19) Cardoso, A. M. S.; Faneca, H.; Almeida, J. A. S.; Pais, A. A. C. C.; Marques, E. F.; de Lima, M. C. P.; Jurado, A. S. Gemini surfactant dimethylene-1,2-bis(tetradecyldimethylammonium bromide)-based gene vectors: A biophysical approach to transfection efficiency. *Biochim. Biophys. Acta, Biomembr.* **2011**, *1808*, 341−351.

(20) Heerklotz, H. Interactions of surfactants with lipid membranes. *Q. Rev. Biophys.* **2008**, *41*, 205−264.

(21) Brito, R. O.; Silva, S. G.; Fernandes, R. M. F.; Marques, E. F.; Enrique-Borges, J.; do Vale, M. L. C. Enhanced interfacial properties of novel amino acid-derived surfactants: Effects of headgroup chemistry and of alkyl chain length and unsaturation. *Colloids Surf., B* **2011**, *86*, 65−70.

(22) Infante, M. R.; Pérez, L.; Pinazo, A.; Clapés, P.; Morán, M. C.; Angelet, M.; García, M. T.; Vinardell, M. P. Amino acid-based surfactants. *C. R. Chim.* **2004**, *7*, 583−592.

(23) Moran, M. C.; Pinazo, A.; Perez, L.; Clapes, P.; Angelet, M.; Garcia, M. T.; Vinardell, M. P.; Infante, M. R. "Green" amino acid-based surfactants. *Green Chem.* **2004**, *6*, 233−240.

(24) Silva, S. G.; Rodríguez-Borges, J. E.; Marques, E. F.; do Vale, M. L. C. Towards novel efficient monomeric surfactants based on serine, tyrosine and 4-hydroxyproline: synthesis and micellization properties. *Tetrahedron* **2009**, *65*, 4156−4164.

(25) Scheuring, S.; Dufrêne, Y. F. Atomic force microscopy: probing the spatial organization, interactions and elasticity of microbial cell envelopes at molecular resolution. *Mol. Microbiol.* **2010**, *75*, 1327−1336.

(26) Garcia-Manyes, S.; Sanz, F. Nanomechanics of lipid bilayers by force spectroscopy with AFM: A perspective. *Biochim. Biophys. Acta, Biomembr.* **2010**, *1798*, 741−749.

(27) Giannotti, M. I.; Vancso, G. J. Interrogation of single synthetic polymer chains and polysaccharides by AFM-based force spectroscopy. *ChemPhysChem.* **2007**, *8*, 2290−2307.

(28) Redondo-Morata, L.; Giannotti, M. I.; Sanz, F. AFM-Based Force-Clamp Monitors Lipid Bilayer Failure Kinetics. *Langmuir* **2012**, *28*, 6403−6410.

(29) Redondo-Morata, L.; Giannotti, M. I.; Sanz, F. In *Atomic Force Microscopy in Liquid: Biological Applications*; Baró, A. M., Reifenberger, R. G., Eds.; Wiley-VCH Verlag & Co. KGaA: Weinheim, Germany, 2012.

(30) Proksch, R.; Schaffer, T. E.; Cleveland, J. P.; Callahan, R. C.; Viani, M. B. Finite optical spot size and position corrections in thermal spring constant calibration. *Nanotechnology* **2004**, *15*, 1344−1350.

(31) Fernandes, R. M. F.; Marques, E. F.; Silva, B. F. B.; Wang, Y. Micellization behavior of a catanionic surfactant with high solubility mismatch: Composition, temperature, and salt effects. *J. Mol. Liq.* **2010**, *157*, 113−118.

(32) Brown, D. A.; London, E. Structure and origin of ordered lipid domains in biological membranes. *J. Membr. Biol.* **1998**, *164*, 103−114.

(33) Correia, R. F.; Viseu, M. I.; Prazeres, T. J. V.; Martinho, J. M. G. Spontaneous vesicles, disks, threadlike and spherical micelles found in the solubilization of DMPC liposomes by the detergent DTAC. *J. Colloid Interface Sci.* **2012**, *379*, 56−63.

(34) Koynova, R.; Tenchov, B. Interactions of surfactants and fatty acids with lipids. *Curr. Opin. Colloid Interface Sci.* **2001**, *6*, 277−286.

(35) Sheikh, K. H.; Giordani, C.; Kilpatrick, J. I.; Jarvis, S. P. Direct Submolecular Scale Imaging of Mesoscale Molecular Order in Supported Dipalmitoylphosphatidylcholine Bilayers. *Langmuir* **2011**, *27*, 3749−3753.

(36) Garcia-Manyes, S.; Oncins, G.; Sanz, F. Effect of Temperature on the Nanomechanics of Lipid Bilayers Studied by Force Spectroscopy. *Biophys. J.* **2005**, *89*, 4261−4274.

(37) Cao, M.; Wang, X.-L. Direct Observation and Distinction of the Inner/Outer Layers of Surfactant Bilayer Formed at the Solid/Solution Interface. *J. Dispersion Sci. Technol.* **2010**, *31*, 38−43.

(38) Li, J. K.; Sullan, R. M. A.; Zou, S. Atomic Force Microscopy Force Mapping in the Study of Supported Lipid Bilayers. *Langmuir* **2011**, *27*, 1308−1313.

(39) Rabinovich, Y. I.; Vakarelski, I. U.; Brown, S. C.; Singh, P. K.; Moudgil, B. M. Mechanical and thermodynamic properties of surfactant aggregates at the solid-liquid interface. *J. Colloid Interface Sci.* **2004**, *270*, 29−36.

(40) Yang, J.; Appleyard, J. The main phase transition of mica-supported phosphatidylcholine membranes. *J. Phys. Chem. B* **2000**, *104*, 8097−8100.

(41) Gurtovenko, A. A.; Patra, M.; Karttunen, M.; Vattulainen, I. Cationic DMPC/DMTAP lipid bilayers: Molecular dynamics study. *Biophys. J.* **2004**, *86*, 3461−3472.

(42) Mbamala, E. C.; Fahr, A.; May, S. Electrostatic model for mixed cationic-zwitterionic lipid bilayers. *Langmuir* **2006**, *22*, 5129−5136.

(43) Bandyopadhyay, S.; Shelley, J. C.; Klein, M. L. Molecular Dynamics Study of the Effect of Surfactant on a Biomembrane. *J. Phys. Chem. B* **2001**, *105*, 5979−5986.

(44) Almeida, J. A. S.; Moran, M. C.; Infante, M. R.; Pais, A. A. C. C. Interaction of arginine-based cationic surfactants with lipid mem-

branes. An experimental and molecular simulation study. *ARKIVOC* **2010**, 34−50.
(45) Garcia-Manyes, S.; Oncins, G.; Redondo, L.; Sanz, F. Nanomechanics of Lipid Bilayers: Heads or Tails? *J . Am. Chem. Soc.* **2010**, *132*, 12874−12886.